Normal alkane evaporation under vacuum: chain-length dependency and distillation from binary systems

Takahashi, Daiki
Horike, Shohei
Koshiba, Yasuko
Ishida, Kenji

(Citation)
Japanese Journal of Applied Physics,61(8):086507

(Issue Date)
2022-08-01

(Resource Type)
journal article

(Version)
Version of Record

(URL)
https://hdl.handle.net/20.500.14094/90009611

REGULAR PAPER • OPEN ACCESS

Normal alkane evaporation under vacuum: chain-length dependency and distillation from binary systems

OPEN ACCESS

Japanese Journal of Applied Physics **61**, 086507 (2022) **REGULAR PAPER**

https://doi.org/10.35848/1347-4065/ac7623

Normal alkane evaporation under vacuum: chain-length dependency and distillation from binary systems

Daiki Takahashi[1], Shohei Horike[1,2,3], Yasuko Koshiba[1,2], and Kenji Ishida[1,2*]

[1]*Department of Chemical Science and Engineering, Graduate School of Engineering, Kobe University, 1-1 Rokkodai-cho, Kobe 657-8501, Japan*
[2]*Membrene and Film Research Center, Kobe University, 1-1 Rokkodai-cho, Kobe 657-8501, Japan*
[3]*PRESTO, Japan Science and Technology Agency, Kawaguchi 332-0012, Japan*

*E-mail: kishida@crystal.kobe-u.ac.jp

Received April 1, 2022; revised May 25, 2022; accepted June 5, 2022; published online July 27, 2022

Normal alkanes are among the simplest molecules that can be studied in physical chemistry. However, there is still more to learn about their liquid-to-gas phase transition characteristics, especially in vacuo. Here, we investigated the evaporation behavior of 12 different normal alkanes using thermogravimetry, both in air and under reduced pressures (5000 to 10^{-2} Pa). The reduced pressures lowered the evaporation-onset temperatures of the normal alkanes. The evaporation-onset temperatures at ~1 Pa were linearly correlated with the chain lengths (molecular weights). Furthermore, we found that the reduced pressures enabled the effective distillation of binary mixtures of normal alkanes because of the differences in the evaporation-onset temperatures. It was empirically determined that distillation (isolated evaporation of one of the binary mixture components) was achieved at ~1 Pa when the chain of one of the alkanes was 30% longer than that of the other.

Supplementary material for this article is available online

1. Introduction

A normal alkane (C_nH_{2n+2}, here denoted as C_n) is an acyclic, unbranched hydrocarbon with sp^3-hybridized carbon atoms and four σ bonds (either carbon–carbon or carbon–hydrogen), as shown in Fig. 1. Normal alkanes have simple chemical structures and nonpolar intermolecular van der Waals interactions, which makes the physical chemistry of their chemical bonding, molecular dynamics, and phase transitions relatively easy to study.[1–3] Their flexibility, hydrophobicity, and aggregating behavior through nonpolar interactions have also been actively exploited in organic chemistry to modify various chemical properties and functions (e.g. solubility and crystallinity) by introducing them as alkyl chains.[4] Further, they have long been an important source of fuel in power stations[5] and plastics manufacturing.[6] In addition, normal alkanes represent the important framework of chain-shaped molecules to create molecular thin films with highly ordered structure by vapor deposition. Several pioneering studies have demonstrated the epitaxial growth of normal alkane on a KCl substrate[7,8] and observed the structure formation by in situ X-ray diffraction during the deposition process.[9] These fabrication and observation techniques provide a useful basis for developing the thin films comprising other functional molecules (e.g. π-conjugated molecules for organic devices).

One of the most interesting physicochemical characteristics of normal alkanes is the dynamics of their phase transitions, such as melting,[10] crystallization,[11] and evaporation.[12] It has widely been recognized that normal alkanes exhibit evenness in their solid−liquid phase transitions[13,14] and that there is a unique rotator phase between the solid and liquid phases.[15,16] Both of these phenomena have been associated with primary molecular structures (conformations and configurations) and intermolecular interactions, and provide insight into the chemical thermodynamics of alkanes.[3–13] The solid−liquid phase transitions of alkanes have also been proposed as a new heat-storage media.[17–19]

The evaporation process (liquid-to-gas phase transition) of alkanes has also been studied for more practical purposes. Petroleum is an important source of alkanes, but it is a mixture of alkanes with various chain lengths.[20,21] The combustion efficiency of alkanes depends on their chain lengths[22]; therefore, petroleum refining by distillation has been historically and technologically a major issue for cost-effective processes in the chemical industry.[23] For the purpose of optimizing the distillation process, thermodynamic properties (e.g. saturation vapor pressures, boiling points, and evaporation enthalpies) have been measured and summarized in a database.[24,25] According to these past studies, longer chain lengths tend to correlate with higher boiling points and evaporation enthalpies for normal alkanes. This tendency seems to be straightforward; the van der Waals force is the dominant intermolecular interaction in these nonpolar materials, and a higher molecular weight results in a stronger van der Waals force. Therefore, a larger amount of heat is necessary for evaporation.

This intensive data collection has been mainly carried out near atmospheric pressure.[24,25] However, petroleum distillation is often performed under vacuum (~2000 Pa),[26] because the reduced external pressure can lower the evaporation temperature. Therefore, it is necessary to obtain the thermophysical properties of normal alkanes by directly measuring their evaporation behavior under vacuum (the pressure conditions of actual refining) to improve the efficiencies of practical processes. Further, the mechanism by which the chain lengths of normal alkanes affect the evaporation process under vacuum, as well as the ideal (or practical) temperature setting for distillation of the alkane mixtures under reduced pressures need further elucidation. Differential scanning calorimetry analysis is useful for measuring solid−liquid phase transitions,[27–30] as it can be performed with

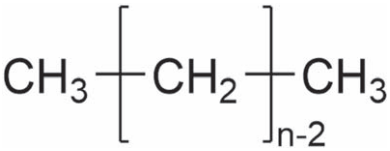

Fig. 1. Chemical structure of normal alkanes.

less material volume change; however, detecting evaporation dynamics is rather difficult because the molecules become gases with large free volume during evaporation or boiling. This difficulty increases when analyzing the evaporation behavior under vacuum.

In this study, we employed thermogravimetric (TG) analysis combined with vacuum pumps to study the evaporation behavior of normal alkanes and their mixtures under vacuum. TG analysis can be used to directly monitor the evaporation dynamics by detecting the material weight loss under a constant heating rate. We confirmed that reduced pressure lowers the evaporation onset temperatures of normal alkanes. It was also revealed that the chain length significantly affects the evaporation behavior of the normal alkane series (n = 20–54). Furthermore, we found that comparing the saturation vapor pressures of two different normal alkanes allowed the determination of the temperature setting for ideal separation by distillation of the binary system of normal alkanes under a certain external pressure (1 Pa).

2. Experimental methods

2.1. Chemicals

We used a series of normal alkanes with different chain lengths. The molecular weight, melting point, and purity are listed in Table I. C24 was supplied by Wako Pure Chemical Industries, C48 and C54 were supplied by Sigma Aldrich, and the other chemicals were supplied by Tokyo Chemical Industry. All the chemicals were used as purchased.

2.2. Setup and measurements

Figure 2 depicts a schematic of the equipment used in the TG measurements (VAP-9000, Advance Riko).[39–42] The system was equipped with a rotary pump and an oil diffusion pump to generate vacuum conditions for studying the evaporation behavior. The rotary pump was used to create a vacuum at a pressure ≧1 Pa. The oil diffusion pump was operated with the rotary pump to create a high vacuum with a pressure <1 Pa. The vacuum level was monitored by a full-range gauge system using a Pirani gauge for low vacuum and a cold cathode gauge under high vacuum. The weight loss in the sample was simultaneously monitored while the sample was heated in an aluminum cell at the rate of 5 °C min^{-1} from room temperature (approximately 25 °C), in presence of an empty reference cell. The initial sample weight was in the range of 10–20 mg. For the measurements of binary mixtures of normal alkanes, C20 powder was combined with C22, C24, or C26 powder. The weight ratio was set to 1:1. The powders were heated to temperatures above the melting points, then cooled to room temperature to obtain homogeneous mixtures before loading into the TG setup.

Table I. Properties of the tested chemicals.

Chemical	Purity (%)	Molecular weight	Melting point (°C)
$C_{20}H_{42}$	>99.5	282.6	36.3[a]
$C_{22}H_{46}$	>99	310.6	44.0[b]
$C_{24}H_{50}$	>97	338.7	54.0[c]
$C_{26}H_{54}$	99.8	366.7	56.4[d]
$C_{28}H_{58}$	>98	394.8	61.1[e]
$C_{30}H_{62}$	>98	422.8	65.5[d]
$C_{36}H_{74}$	98.7	507.0	75.6[f]
$C_{40}H_{82}$	>97	563.1	80.0[f]
$C_{44}H_{90}$	>97	619.2	85.3[f]
$C_{48}H_{98}$	>98	675.3	87.5–88.5[g]
$C_{50}H_{102}$	>98	703.4	93.0[h]
$C_{54}H_{110}$	>98	759.5	94.4[i]

a) From A. Genovese et al.[31] b) From D. Ivanov et al.[32] c) From G. Gillet et al.[33] d) From A. W. Schmidt et al.[34] e) From S. Hafsaoui et al.[35] f) From L. Ventola et al.[36] g) From G. Schill et al.[37] h) From F. S. Sinnatt et al.[38] i) From our data using differential scanning calorimetry (for more details, see supporting information).

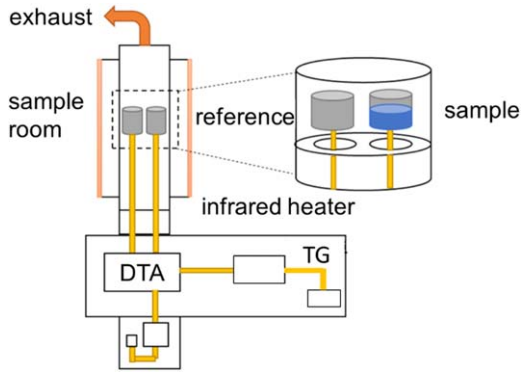

Fig. 2. (Color online) Schematic of TG setup equipped with vacuum pumps and a vacuum gauge.

2.3. Data analysis

The evaporation onset temperature was defined as the temperature at which the weight decreased by 5%, with respect to the purity of the neat powders and the weight-loss resolution of the setup. The evaporation rate r is expressed as:

$$r = -\frac{1}{U} \cdot \frac{d\Delta W}{dt}. \quad (1)$$

Here, U is the cross-sectional area of the sample cell (1.40×10^{-5} m^2), ΔW is the weight loss, and t is the time. The $d\Delta W/dt$ term was calculated using the least-square method. To investigate the applicability of distillation for normal-alkane binary systems, the saturation vapor pressure P was calculated from the evaporation rates using the Hertz–Knudsen–Langmuir equation:[43,44]

$$\alpha P = r\sqrt{\frac{2\pi RT}{M}}. \quad (2)$$

Here, α ($0 < \alpha \leqq 1$) is the coagulation factor, R (8.31 J K^{-1} mol^{-1}) is the gas constant, T is the temperature, and M is the molecular weight. α represents the degree of evaporation hindrance by residual gas molecules; therefore, it has different values depending on the external pressure. Here, we consider that the value of α is an apparatus constant that does not depend on the type of material.[45] Thus, we used the αP values to compare the vapor pressures of the normal alkanes.

3. Results and discussion

3.1. Vacuum level and chain length dependencies

We first studied the evaporation behavior of C20, a normal alkane with the shortest chain length tested in this study,

under various pressures [Fig. 3(a)]. The weight-loss onset temperature decreased at a higher vacuum level: 191.0 °C in air, 142.0 °C at 5.0×10^3 Pa, 73.3 °C at 1.0 Pa, and 67.8 °C at 1.8×10^{-2} Pa. These onset temperatures are much higher than the melting point of C20 (see Table I); therefore, the observed weight losses are due to evaporation, not sublimation. Residual gas molecules (e.g. nitrogen and oxygen) surrounding the liquid hinder liquid evaporation. Therefore, the reduced pressure contributed to liquid evaporation at a lower temperature.

Next, we compared the evaporation behaviors of a series of normal alkanes (C20–C54) using TG measurements both in air and under vacuum (∼1 Pa), as shown in Figs. 3(b)–3(c). For all the samples, the onset temperature of weight loss decreased under reduced pressure. Further, the onset temperature increased as the chain length increased (note that evaporation is also responsible for these weight losses, because the onset temperature is higher than each melting point, as listed in Table I). The increase in the onset temperature is logical because the longer chain length (higher molecular weight) corresponds to stronger intermolecular van der Waals interactions, which increase the thermal energy required for evaporation. Interestingly, the evaporation onset temperatures linearly increased according to the carbon number, as shown in Fig. 3(d). Based on these linearities, we derived relationships between the evaporation onset temperature T_{onset} in air and at an external pressure of 1 Pa and the number of carbons (or molecular weight) as follows:

$$T_{\mathrm{onset}}^{\mathrm{air}} = 5.66 \times n + 87.67, \tag{3}$$

$$T_{\mathrm{onset}}^{1\ \mathrm{Pa}} = 5.62 \times n - 40.85, \tag{4}$$

which can be used to estimate the evaporation onset temperature in air and at 1 Pa. As the evaporation onset temperature is an arbitrary parameter (herein, the temperature at which the weight loss reaches −5% detected by the TG setup), Eqs. (3) and (4) should be regarded as technically useful relations. However, boiling points (thermodynamical or physicochemical parameter) of normal alkanes have a similar linear relation depending on the carbon number (for more details, see Fig. S2 (available online at stacks.iop.org/JJAP/61/086507/mmedia) of supplementary data). Our measurements reveal that this linearity remains valid even using such arbitrary weight loss onset temperature as a parameter. The applicability of Eqs. (3) and (4) is currently limited to the chain length range n = 20–54. There is a possibility of extending this to normal alkanes with other chain lengths, as well as other vacuum levels, by applying similar measurements in the future.

3.2. Separating binary systems by distillation

We then investigated the evaporation behavior of normal alkanes in equal-mass mixtures with various chain lengths. The different evaporation onset temperatures of the normal alkanes with different chain lengths under vacuum, shown in Figs. 3(b) and 3(c), immediately suggested the applicability of distillation to these mixtures. To verify this possibility, C20 was combined with C22, C24, or C26, and the evaporation-onset temperature and vapor pressure were measured. Figures 4(a) and 4(b) show the TG curve for

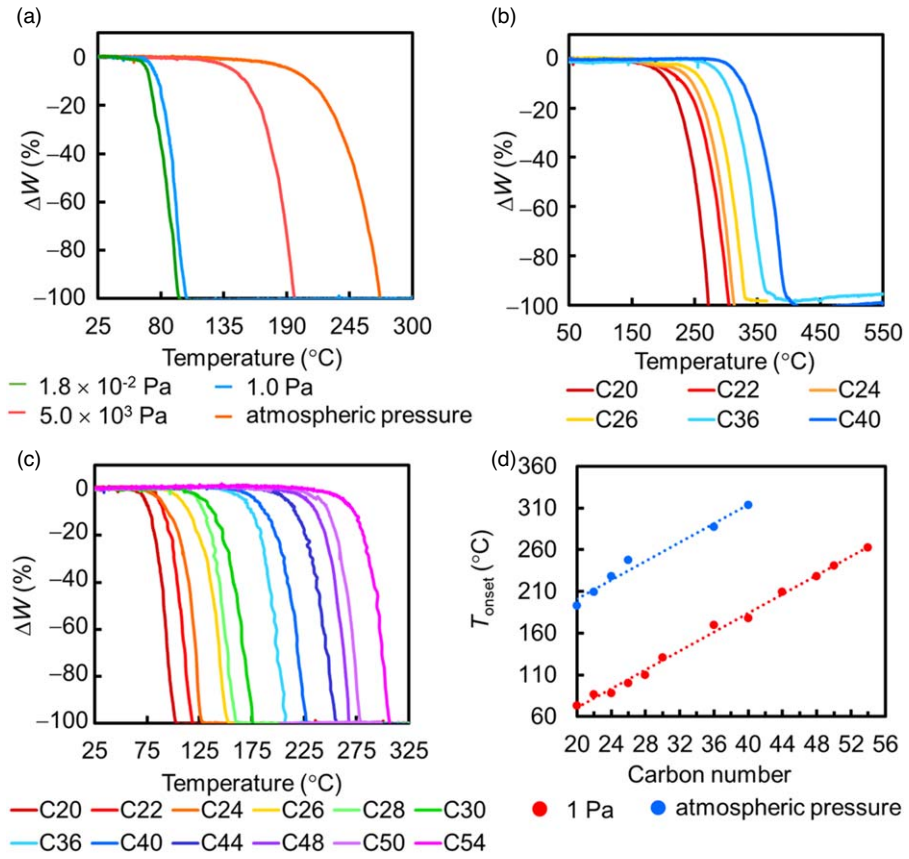

Fig. 3. (Color online) (a) TG data under various pressures. TG data for normal alkanes with various chain lengths, (b) in air, and (c) under vacuum (∼1 Pa). (d) Correlations of evaporation onset temperature of normal alkanes with the chain length (the number of carbons) in air and under vacuum (∼1 Pa).

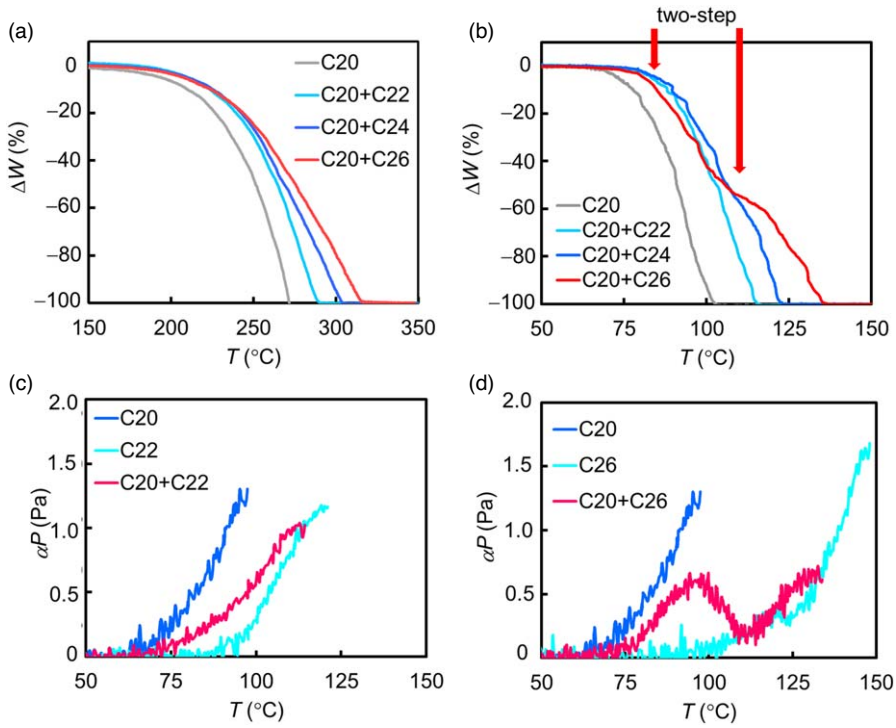

Fig. 4. (Color online) TG data of equal-mass mixtures of C20 combined with C22, C24, or C26 measured (a) in air and (b) under vacuum (∼1 Pa). Saturation vapor pressures (in terms of αP) of (c) C20/C22 and (d) C20/C26 systems calculated from Eq. (2) using TG data obtained at ∼1 Pa. Note that the absolute values of $\alpha\beta p$ cannot be compared for these mixtures in the present case because the molecular weight in Eq. (2) is the average value of each component (296.6 for C20/C22 and 324.6 for C20/C26) for the mixtures. Thus, the shapes of plots are discussed for investigating the possibility of distillation.

each mixture along with that of neat C20 observed in air and under vacuum (∼1 Pa), respectively. The weight-loss onset temperature in air was higher than that of neat C20 when C20 was combined with alkanes with a longer chain length, as shown in Fig. 4(a). The one-step weight loss behavior of the mixtures directly indicates that alkanes with different chain lengths evaporated simultaneously, not separately. In this case, intermolecular interactions between the identical normal alkanes (i.e. C20/C20), as well as pairs of alkanes with different chain lengths (i.e. C20/C22, C20/C24, and C20/C26), were considered to contribute to the evaporation onset temperatures. As depicted in Figs. 3(b) and 3(c), the longer chain length (higher molecular weight), correlates with stronger intermolecular van der Waals forces, and a higher evaporation onset temperature. Therefore, mixing C20 with normal alkanes with longer chain lengths increased the energy required for evaporation compared to neat C20. This was due to stronger intermolecular interactions with C22, C24, and C26 than with identical C20. It should be noted that the one-step weight loss behaviors indicate that each component in the 3 tested combinations of binary mixtures cannot be separated by distillation in air.

As shown in Fig. 4(b), this behavior changes under vacuum (∼1 Pa): the binary mixture of C20 and C26 shows a clear two-step weight loss, whereas those of the other mixtures (C20/C22 and C20/C24) still show one-step weight losses, with slightly increased evaporation-onset temperatures compared to that of neat C20. The first step of the weight loss from the C20/C26 system is completed at $\Delta W = -50\%$, and the remaining 50% of the sample evaporates in the second step. Since the binary system is composed of an equal-mass mixture of C20 and C26, and the evaporation-onset temperature of C26 is much higher (∼33 °C) than that of C20, as shown in Fig. 4(b), it is apparent that the C20 component evaporated in the first step, then the residual C26 evaporated in the second step. According to previous reports on the interface between crystals of normal alkanes with different chain lengths, the molecules diffuse across the crystal interface.[46] Owing to such a high degree of molecular compatibility, the normal alkanes in the binary mixtures should be well dispersed in their melt states (photographs of the melts can be seen in Fig. S3 of supplementary data). Note that the TG curve of the sample obtained from the solidified mixture from the melts was nearly identical with that of the equal-mass mixture of C20/C26 shown in Fig. 4(b), which further supports the good affinity of each component). Therefore, the observed two-step weight loss was not caused by phase separation in the liquid phase associated with the difference in densities. This conclusion clearly indicates that distillation can be applied to mixtures of C20 and C26 under reduced pressure (∼1 Pa). In contrast, the other two mixtures (C20/C22 and C20/C24) could not be separated by distillation owing to the relatively similar evaporation onset temperature of each component at 1 Pa. In general, distillation would be more efficient under vacuum than in air. The slope of the TG curve (corresponding to evaporation rate) becomes steeper with the increase in vacuum level as shown in Fig. 3(a), which results in the complete evaporation of one component with higher volatility (in the present case, C20) below the onset temperature of the other (e.g. C26).

The applicability of distillation to a binary mixture according to the combined chain lengths can be readily understood by comparing the vapor pressure of each component. Figures 4(c) and 4(d) show the saturation vapor pressures (in terms of αP) of equal-mass mixtures of C20/C22 and C20/C26 under vacuum (∼1 Pa), respectively. The

vapor pressure of neat C20 starts to increase at approximately 66 °C, while those of neat C22 and C26 start to increase at ∼90 °C and ∼105 °C, respectively. For the mixtures of C20/C22 and C20/C26, the onset temperatures of the vapor pressure difference became ∼75 °C (slightly higher than that of neat C20) owing to the slight shifts in the evaporation onset temperature, as shown in Figs. 4(a) and 4(b). Notably, the vapor pressure of the C20/C26 mixture decreased at ∼98 °C, and then increased again at ∼112 °C. This behavior corresponds to the two-step weight loss in the TG curve shown in Fig. 4(b), and the temperature-dependent vapor pressures of C20 and C26. Since the vapor pressure of C26 is still close to 0 Pa at ∼90 °C, while that of C20 takes on a finite value, this temperature is suitable at ∼1 Pa for separating these components by removing C20 only. In contrast, the vapor pressure of the C20/C22 mixture could not be distinguished into each contribution, which corresponds to the one-step weight loss in Fig. 4(b) and the difficulty of separating each component by distillation. Therefore, our measurement setup and data analysis approach has great potential to provide information on the temperature setting for distillation under a certain external pressure. The applicability of distillation to the C20/C26 system is not limited to the equal-mass mixture. Figure 5 shows the TG curves of the mixtures in which C20 and C26 were mixed at ratios of 1:1, 3:1, and 1:3. For all the mixed ratios, the two-step weight loss is consistent with the initial weight of C20, which further supports the isolated evaporation of the components and the feasibility of separation.

Based on the above discussion, the difference in chain lengths ($\Delta n = n_2 - n_1$, $n_2 > n_1$) should be considered to predict the applicability of distillation to binary mixtures of normal alkanes (two-step weight loss in TG and vapor-pressure difference according to temperature). To further investigate this consideration, we performed TG measurements for equal-mass mixtures of C30 with C36, C40, or C44 at ∼1 Pa, as shown in Fig. 6. The C30/C40 ($\Delta n = 10$) and C30/C44 ($\Delta n = 14$) binary systems exhibited clear two-step weight losses, whereas only one-step weight loss was observed for the mixture of C30 and C36 ($\Delta n = 6$). For the binary mixtures containing C20, at least $\Delta n = 6$ was required to realize the two-step weight loss (C20/C26 system) at ∼1 Pa, as shown in Fig. 4(b), which does not agree with the Δn required to realize the two-step weight loss in the C30/Cn_2 systems, because $\Delta n = 6$ is insufficient for separation of the C30 and Cn_2 components. Although Δn itself corresponds to the difference in the evaporation onset temperatures between the two normal alkanes, as expressed by Eq. (3), this value does not seem to be directly correlated with the appearance of isolated evaporation of each component. Here, we empirically found that the two-step weight loss (isolated evaporation of each component) could be realized in binary mixtures of normal alkanes with different chain lengths (n_1 and n_2) when they meet the relation of $\Delta n/n_1 > 0.3$ (n_2 must be at least 30% larger than n_1). The implication of the value 0.3 is unclear at this stage; however, the isolated evaporation of normal alkanes from their binary mixtures seems to be affected by not only the difference in evaporation onset temperature between each component (determined by the molecular weight of Cn_1 and Cn_2) but also by the intermolecular interactions (either Cn_1/Cn_1 or Cn_1/Cn_2). For example, the evaporation onset temperatures of the mixtures of C20 with C22, C24, and C26 are higher than that of pure C20. The presence of the longer alkanes with the higher molecular weights (C22, C24, or C26) may suppress the evaporation due to the occurrence of stronger van der Waals intermolecular interactions than that between the C20/C20 system. This implies that the former effect must sufficiently exceed the latter effect to realize isolated evaporations. In summary, our method (TG measurement under vacuum) can provide a useful baseline for analyzing the evaporation behaviors of normal alkanes, as well as their mixtures, in terms of evaporation-onset temperature, and the applicability of distillation.

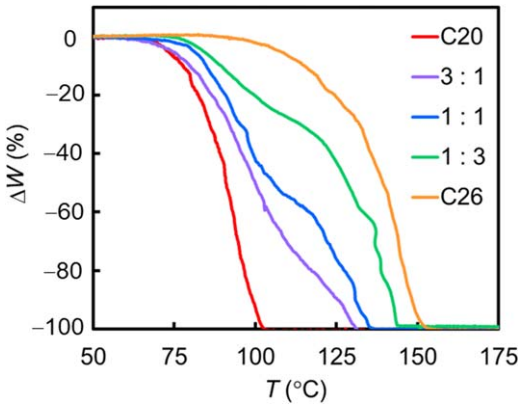

Fig. 5. (Color online) TG data of C20/C26 mixtures with different weight ratios measured under vacuum (∼1 Pa).

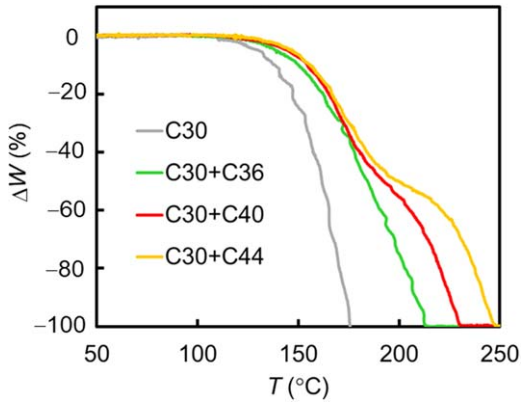

Fig. 6. (Color online) TG data of equal-mass mixtures of C30 combined with C36, C40, and C44 measured at ∼1 Pa.

4. Conclusions

We studied the evaporation of normal alkanes under vacuum using TG measurements. The weight-loss onset temperatures were higher than the melting points of the alkanes, which indicates that the weight loss was due to evaporation, not sublimation. The evaporation onset temperature decreased with increasing vacuum level. Normal alkanes with longer chain lengths evaporated at higher temperatures because of stronger intermolecular interactions. The evaporation onset temperature at ∼1 Pa was linearly correlated with the chain length (molecular weight), which allowed us to derive an equation for estimating the onset temperature from the chain length. For binary mixtures of normal alkanes with various chain lengths, the evaporation behavior (one-step or two-step

weight loss) was correlated to the difference between the chain lengths of each component: two-step weight loss (isolated evaporation of each component) was observed when the chain-length difference between each component was large, while only one-step weight loss (simultaneous evaporation of both components) was observed when alkanes with similar chain lengths were evaporated. The two-step weight-loss behavior clearly corresponds to the applicability of the distillation process to these combined alkane mixtures. We empirically found that isolated evaporation of each component occurred in cases where $(n_2–n_1)/n_1 > 0.3$ $(n_2 > n_1)$ at an external pressure of 1 Pa. The present study is limited to even-numbered normal alkanes; evaporation behaviors of odd-numbered alkanes will be investigated in future studies. Further, our concepts of measurement and data analysis can be extended to other organic molecules and their mixtures and may be useful for cost-effective and eco-friendly distillation in the petroleum and chemical industries. In particular, alkanes with branched or cyclic structures will be the next research targets in our work to understand the effects of primary molecular structures and intermolecular interactions on evaporation and distillation processes. Although the melts of the binary mixtures of alkanes are macroscopically homogeneous without any phase separations, the surface-covering of each component may be another important factor to consider while discussing the changes in evaporation onset temperature, rate, and the applicability of distillation for the mixtures because the evaporation should occur at the surface of the liquids; this will be addressed in our future study.

Acknowledgments

This work was supported in part by JST CREST and JSPS KAKENHI. S.H. would like to thank JST PRESTO.

ORCID iDs

Shohei Horike https://orcid.org/0000-0002-9656-0103
Yasuko Koshiba https://orcid.org/0000-0001-7189-0109
Kenji Ishida https://orcid.org/0000-0003-1227-9638

1) C. W. Bunn, Trans. Faraday Soc. **35**, 482 (1939).
2) J. P. Rabe and S. Buchholz, Science **253**, 424 (1991).
3) N. F. M. Branco, A. I. M. C. Lobo Ferreira, J. C. Ribeiro, L. M. N. B. F. Santos, and J. A. P. Coutinho, Fuel **262**, 116488 (2020).
4) H. W. Sternberg, C. L. Delle Donne, P. Pantages, E. C. Moroni, and R. E. Markby, Fuel **50**, 432 (1971).
5) K. Guo, H. Li, and Z. Yu, Fuel **185**, 886 (2016).
6) R. T. S. Bernd, M. M. Patricia, and M. D. Borys, Environ. Sci. Technol. **39**, 6961 (2005).
7) M. Ashida, Y. Ueda, and H. Yanagi, Bull. Chem. Soc. Jpn. **59**, 1437 (1986).
8) Y. Ueda, Bull. Chem. Soc. Jpn. **60**, 2011 (1987).
9) K. Hayashi, K. Ishida, T. Horiuchi, and K. Matsushige, Jpn. J. Appl. Phys. **31**, 4081 (1992).
10) L. Mandelkern, A. Prasad, and R. G. Alamo, Macromolecules **23**, 3696 (1990).
11) M. Dirand, M. Bouroukba, V. Chevallier, D. Petitjean, E. Behar, and V. Ruffier-Meray, J. Chem. Eng. **47**, 115 (2002).
12) H. Sakurai, H. J. Tobias, K. Park, D. Zarling, K. S. Docherty, D. B. Kittelson, P. H. McMurry, and P. J. Ziemann, Atomos. Environ. **37**, 1199 (2003).
13) E. B. Sirota, A. B. Herhold, H. Gang, and H. H. Shao, AlChE1999 Spring Natl. Meeting **58a**, 107 (1999).
14) A. Müller, Proc. R. Soc. A **124**, 317 (1929).
15) J. Doucet, I. Denicolo, and A. F. Creievich, J. Chem. Phys. **75**, 1523 (1981).
16) D. L. Dorset, B. Moss, J. C. Wittmann, and B. Lotz, Proc. Natl Acad. Sci. USA **81**, 1913 (1984).
17) P. Espeau, L. Robles, D. Mondieig, Y. Haget, and M. A. Cuevas-Diarte, "J. Ll," Tamarit, Mater. Res. Bull. **31**, 1219 (1996).
18) D. Mondieig, F. Rajabalee, A. Laprie, H. A. J. Oonk, T. Calvet, and M. A. Cuevas-Diarte, Transfus. Apheris Sci. **28**, 143 (2003).
19) L. Ventolà, T. Calvet, M. A. Cuevas-Diarte, V. Métivaud, D. Mondieig, and H. A. J. Oonk, Mater. Res. Innovations **6**, 284 (2002).
20) H. de Jonge, J. I. Freijer, J. M. Verstraten, J. Westerveld, and F. W. M. van der Wielen, Environ. Sci. Technol. **31**, 771 (1997).
21) L. Mansuy, R. Paul Philip, and J. Allen, Environ. Sci. Technol. **31**, 3417 (1997).
22) C. Yuan, D. A. Emelianov, M. A. Varfolomeev, W. F. Pu, and A. S. Ushakova, Energy Fuel **32**, 7933 (2018).
23) G. Bovzkaj, A. Przyjazny, and M. Kaminski, Anal. Bioanal. Chem. **399**, 3253 (2011).
24) D. L. Morgan and R. Kobayashi, Fluid Phase Equilib. **97**, 211 (1994).
25) A. P. Kudvhadker and B. J. Zwolinski, J. Chem. Eng. Data **11**, 253 (1966).
26) W. Gu, Y. Huang, K. Wang, B. Zhang, Q. Chen, and C. W. Hui, Energy **76**, 559 (2014).
27) T. Shen, H. Peng, and X. Ling, Lnd. Eng. Chem. Res. **58**, 15026 (2019).
28) M. R. Pallaka, D. K. Unruh, and S. L. Simon, Athermochimica Acta **663**, 157 (2018).
29) G. W. H. Höhne, Thermochim. Acta **332**, 115 (1999).
30) M. J. Oliver and P. D. Calvert, J. Cryst. Growth **30**, 343 (1975).
31) A. Genovese, G. Amarasinghe, M. Glewis, D. Mainwaring, and A. R. Shanks, Thermochim. Acta **443**, 235 (2006).
32) D. Ivanov, B. Stroianova-Ivanova, and C. Ivanov, Doklady Bolgarskoi Akademii Nauk **8**, 33 (1955).
33) G. Gillet, O. Vitrac, and S. Desobry, Ind. Eng. Chem. Res. **48**, 5285 (2009).
34) A. Schmidt, V. Schoeller, and K. Eberlein, Berichte der Deutschen Chemischen Gesellschaft [Abteilung] B: Abhandlungen **74B**, 1313 (1941).
35) S. L. Hafsaoui and R. Mahmoud, J. Therm. Anal. Calorim. **88**, 565 (2007).
36) L. Ventola, M. A. Cuevas-Diaarte, T. Calvet, I. Angulo, M. Bernar, G. Bernar, M. Melero, and D. Mondieig, J. Phys. Chem. Solids **66**, 1668 (2005).
37) G. Schill, C. Zuercher, and H. Fritz, Chem. Ber. **111**, 2901 (1978).
38) N. I. Chernozhukov, V. V. Vainshtok, and B. N. Kartinin, Izv. Vysshikh Uchebnykh Sevedenii, Neft I Gaz **11**, 481 (1962).
39) S. Horike, M. Ayano, M. Tsuno, T. Fukushima, Y. Koshiba, M. Misaki, and K. Ishida, Phys. Chem. Chem. Phys. **20**, 21262 (2018).
40) Y. Koshiba, M. Nishimoto, A. Misawa, M. Misaki, and K. Ishida, Jpn. J. Appl. Phys. **55**, 03DD07 (2015).
41) M. Yamada, Y. Koshiba, S. Horike, T. Fukushima, and K. Ishida, Jpn. J. Appl. Phys. **59**, SDDA15 (2019).
42) K. Yase, Y. Takahashi, N. Ara-kato, and A. Kawazu, Jpn. J. Appl. Phys. **34**, 636 (1995).
43) I. Langmuir, Phys. Rev. **2**, 329 (1913).
44) Y. Takahashi, K. Matsuzaki, M. Iijima, E. Fukuda, S. Tsukahara, Y. Murakami, and A. Maesono, Jpn. J. Appl. Phys. **32**, 875 (1993).
45) R. Littlewood and E. Rideal, Trans. Faraday Soc. **52**, 1598 (1956).
46) T. Yamamoto, H. Aoki, S. Miyaji, and K. Nozaki, Polymer **38**, 2643 (1997).